

The Simple Cubic Structure of Ruthenium Clusters

Wenqin Zhang,^{†,‡} Haitao Zhao,[†] and Lichang Wang^{*,‡}

Department of Chemistry and State Key Laboratory of C1 Chemical Technology, Tianjin University, Tianjin, 300072, P. R. China, and Department of Chemistry and Biochemistry, Southern Illinois University, Carbondale, Illinois 62901

Received: July 10, 2003; In Final Form: December 4, 2003

Ruthenium clusters of up to 64 atoms were studied using density-functional theory with a plane wave basis set. The simple cubic structure was found to be the most stable structure in the formation of small ruthenium clusters. A strong trend of trimer formation was also observed in the linear ruthenium clusters. All the ruthenium clusters investigated in this work are ferromagnetic with large magnetic moments and have small energy gaps between the highest occupied and the lowest unoccupied molecular orbitals. A quantitative correlation was established between the energetic, electronic, and magnetic properties of ruthenium clusters and the cluster size and structure. Our analysis showed that the atoms in similar bonding environments have similar binding energies. On the basis of this analysis, estimations were made on the binding energy for certain planar and simple cubic ruthenium clusters. The estimated binding energies are in good agreement with those from the density-functional theory calculations.

1. Introduction

Ruthenium clusters have been attractive research subjects because of their roles as catalysts and the complexity of their spin multiplicities that result in various interesting electronic and magnetic properties. Ruthenium dimer was investigated extensively both experimentally^{1,2} and theoretically.^{3–8} Bond distances of 224–271 pm and binding energies of 0.64–5.04 eV/atom were reported from various studies on the dimer.^{1–8} Guo and Balasubramanian⁹ calculated the electronic states of the Ru trimer, Ru₃, at the highest MRSDCI level and found that the ground state of Ru₃ is ¹¹B₂ with isosceles triangular geometry. However, a bond length of 391.9 pm for the trimer is too long.

In addition to the dimer and trimer, other small ruthenium clusters, especially the 13-atom clusters, Ru₁₃, and the 55-atom clusters, Ru₅₅, were studied theoretically.^{9–18} Wang et al. investigated the Ru₁₃ clusters with *I_h*, *O_h*, and *D_{3h}* symmetries using the discrete-variation local spin-density-functional method.^{11,12} It was found that the *I_h* symmetry Ru₁₃ cluster has a bond distance of 254 pm and is the most stable structure with a binding energy of 5.23 eV/atom. This cluster has a magnetic moment of 0.31 μ_B /atom. Guirado-López and co-workers studied the structural effects on the magnetism of small Ru clusters using a tight-binding Hubbard Hamiltonian in the unrestricted Hartree–Fock approximation.^{13,14} They found that the magnetic moments of those ruthenium clusters vary from 0 to 1.135 μ_B /atom. Their calculations also showed that the binding energy increases from 3.3 eV/atom for the Ru₅ cluster to 4.28 eV/atom for the ruthenium bulk. Furthermore, Reddy et al. calculated the magnetic moments for the icosahedral and cubo-octahedral Ru₁₃ clusters as 0.92 μ_B /atom and 1.08 μ_B /atom, respectively.¹⁵ Wildberger et al. performed local density-functional theory calculations and applied a KKR Green's function method to

study the magnetic characters of one- and two-dimensional Ru clusters deposited on the Ag(001) surface.¹⁶ They reported that the square-shaped Ru₄ and Ru₉ clusters are strongly ferromagnetic with magnetic moments of 1.8 and 1.4 μ_B /atom, respectively. In contrast, Cox et al. found that Ru clusters are almost nonmagnetic with the highest magnetic moment for the Ru₁₀ cluster <0.32 μ_B /atom.¹⁷

Despite those studies, there are no systematic investigations on ruthenium clusters, which is critical for correlating the catalytic behaviors of ruthenium clusters with their properties. Furthermore, it is dangerous to predict the most stable isomers because only a limited number of isomers have been studied so far. For instance, to the best of our knowledge, all the publications^{11–14} showed that the Ru₁₃ cluster with *I_h* symmetry is the most stable structure among 13-atom clusters. The results from the current study, however, show that this is incorrect.

Therefore, a systematic investigation of the ruthenium clusters was carried out using density-functional theory (DFT) with a plane wave basis set. We obtained the energetic and electromagnetic properties for more than 60 Ru clusters. These results allowed us to correlate how the properties of Ru clusters depend on the cluster size and structure, as the properties of transition metal clusters were found to be strongly dependent on the cluster size and structure.^{19,20}

In what follows, we first briefly summarize the methodology of our calculations and provide numerical details in section 2. We then present the results and discussion in section 3. Finally, conclusions are drawn in section 4.

2. Method

Our calculations were carried out using DFT with a plane wave basis set, which was implemented in VASP (Vienna ab initio simulation package).^{21–23} The electron–ion interaction was described by optimized ultrasoft pseudopotentials²⁴ with a cutoff energy of 300 eV. The exchange and correlation energies were calculated using the Perdew–Wang 91 form of the generalized gradient approximation (GGA).²⁵

* Author to whom correspondence should be addressed. E-mail: lwang@chem.siu.edu. Phone: 618-453-6476. Fax: 618-453-6408.

[†] Tianjin University.

[‡] Southern Illinois University.

Over 60 Ru clusters were investigated in this work. There are many energetically possible isomers at large cluster sizes, and only a limited number of them were chosen. Our choice of these isomers was made according to the stable structures of small Ru clusters and the stable building blocks that were found among smaller Ru clusters from our calculations. The initial structures were set in their highest possible symmetry with reasonable bond distances of 2–2.3 Å, 2.2–2.5 Å, and 2.3–2.7 Å for the linear, planar, and three-dimensional Ru clusters, respectively. A full geometry optimization was used to minimize the total energy of the cluster without imposing the initial symmetry constraint. We note that the relaxed Ru clusters depend more sensitively on the initial choice of the bond distances than the Rh, Pd, Ir, and Pt clusters that we studied previously.^{26–28} When multiple results were obtained for the same initial structure but different initial bond distances, we chose the most stable one as the ground state.

In addition to the bond distances, we calculated the binding energy, the energy difference between the highest occupied molecular orbital (HOMO) and the lowest unoccupied molecular orbital (LUMO), that is, the HOMO–LUMO band gap (E_G), and the magnetic moment for the Ru clusters. The binding energy per atom (E_B) was calculated by

$$E_B = (NE_{\text{atom}} - E_{\text{cluster}})/N \quad (1)$$

where E_{atom} and E_{cluster} are the total energies (in eV) of an isolated Ru atom and of the cluster, respectively. We use N to represent the number of atoms in the cluster. The unit of E_B is eV/atom. The magnetic moment per atom (μ) was calculated by

$$\mu = (S_u - S_d)/N \quad (2)$$

where S_u and S_d are the number of electrons with the majority and the minority spins, respectively. The unit of μ is μ_B/atom . In the following, we will refer to the binding energy per atom as the binding energy and the magnetic moment per atom as the magnetic moment for convenience of presentation.

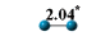
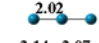
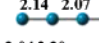
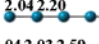
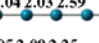
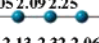
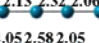


3. Results and Discussion

To clarify our presentation, we use L_N , iP_N , and iT_N to represent the linear, planar, and three-dimensional Ru clusters, respectively, where the subscript N is the number of atoms in the cluster (also denoted as cluster size) and the superscript i is the i th isomer at a given cluster size and dimensionality. In what follows, we start our discussion from the linear Ru clusters.

3.1. Linear Ru Clusters. Nine linear Ru clusters were investigated together with an infinite linear cluster for comparison. The calculated binding energies, the HOMO–LUMO band gaps, and the magnetic moments of these clusters are given in Table 1.

Before we discuss the results obtained for the linear Ru clusters, we first compare our results for the Ru dimer, L_2 , with those in the literature. The binding energy of 2.02 eV/atom from the current calculation is in excellent agreement with the experimental value of 2.0 ± 0.2 eV/atom,² the value of 2.0 eV/atom from the CAS–MCSCF calculation⁵ and the MRSDCI calculation,⁸ and the value of 2.20 eV/atom from the B3LYP calculation.⁸ But our result is larger than the value of 0.59 eV/atom obtained from the DFT calculation with an all-electron Gaussian basis set⁷ or the value of 1.29 eV/atom obtained from the norm-conserving pseudopotential DFT.⁷ Our calculation shows that the bond length of L_2 is 2.04 Å, which is shorter than those of 2.24–2.71 Å from the previous calculations.^{3–8}

TABLE 1: Bond Distances, Binding Energies (E_B), HOMO–LUMO Band Gaps (E_G), and Magnetic Moments (μ) of Linear Ru Clusters

Notation	Structure ($D_{\infty h}$)	E_B (eV/atom)	E_G (eV)	μ (μ_B/atom)
L_2		2.02	0.43	2.00
L_3		2.50	0.33	0.67
L_4		2.45	1.19	1.50
L_5		2.58	0.35	1.20
L_6		2.70	0.24	0.67
L_7		2.69	0.32	0.29
L_8		2.70	0.26	0.50
L_9		2.75	0.42	0.89
L_{∞}		2.88	0.24	0.91

*The bond distance is in angstroms. The unlabeled bonds have the same values as their corresponding symmetric bonds.

Our calculated ground state of L_2 is quintet, which is different from the ${}^7\Delta_u$ (${}^7\Sigma$) state obtained previously.^{3–5,7,8} We also obtained a Ru dimer with a magnetic moment of 4.0 μ_B/atom and a bond length of 2.21 Å, but its binding energy is 0.21 eV/atom less than that of the L_2 in Table 1.

The most striking observation of the linear Ru clusters in Table 1 is the periodical alternation of two short bonds and one long bond in L_6 and L_9 as well as the relatively larger binding energies of L_3 , L_6 , and L_9 . These results indicate that linear Ru clusters tend to form trimers, which results in $3 \times n$ wires, such as the more stable L_3 ($n = 1$), L_6 ($n = 2$), and L_9 ($n = 3$). This trimer formation in the linear Ru clusters is similar to the well-known H_2 dimer formation when one aligns H atoms linearly. It also explains why the binding energy of the Ru trimer is 87% of that of the infinite linear Ru structure, L_{∞} , whereas the binding energy of the Pd trimer is only 67% of that of the infinite linear Pd structure.²⁷

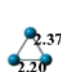
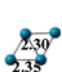

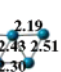
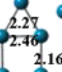
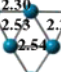
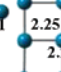
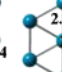
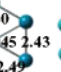
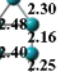
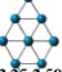
The bond distances of most linear Ru clusters are, as we expected, shorter than the value of the Ru bulk (2.65 Å from ref 29 and 2.70 Å calculated here). The binding energy of the infinite linear Ru, L_{∞} , is 43% of the value of the Ru bulk, whereas it is 33% for the Pd.²⁷ These results indicate that the linear Ru wires are relatively more stable than the Pd wires.

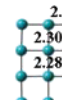
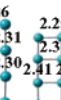
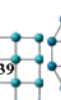
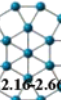
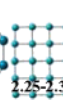
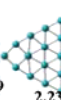
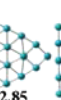
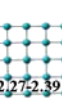
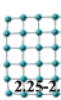
Except for the Ru tetramer, L_4 , the band gaps of the linear Ru clusters are rather small, as shown in Table 1. This indicates that the Ru wires are good electrical conductors. Furthermore, the results in Table 1 illustrate that the Ru wires are ferromagnetic. This agrees well with the ab initio results on the Ru clusters deposited on the Ag(001) surface where the linear Ru_2 , Ru_3 , and Ru_4 were found to have magnetic moments as large as 2.2 μ_B/atom and both the inner and outer chain atoms have about the same moment.¹⁶

3.2. Planar Ru Clusters. The structural information, binding energies, HOMO–LUMO band gaps, and magnetic moments of eighteen planar ruthenium clusters up to 36 atoms are summarized in Table 2. The information on two infinite planar Ru clusters is also provided there.

The Ru trimer was studied previously.^{9,10,16,30} Fang et al. measured the Raman spectra of the Ru_3 in argon matrixes without the detection of its geometry.¹⁰ Guo and Balasubramanian reported that the ground state of the Ru trimer is an isosceles triangle with bond lengths of 2.673 and 3.919 Å.⁹ We did a single-point calculation with this geometry and our results show that the binding energy is 1.84 eV/atom. The relaxed Ru trimer from the same input as the single-point calculation has

TABLE 2: Bond Distances (in Å), Binding Energies (E_B), HOMO–LUMO Band Gaps (E_G), and Magnetic Moments (μ) of Planar Ru Clusters

Notation	P ₃	¹ P ₄	² P ₄ [*]	¹ P ₅	² P ₅	¹ P ₆	² P ₆	¹ P ₇	² P ₇	¹ P ₉	² P ₉
Structure											
Symmetry	C _{2v}	C _{2h}	D _{4h}	C _{2v}	C _{2v}	C _{2v}	D _{2h}	D _{2h}	C _{2v}	C _{2h}	D _{4h}
E _B (eV/atom)	2.59	2.73	3.09	2.89	3.20	3.05	3.32	3.28	3.35	3.39	3.59
E _G (eV)	0.41	0.13	0.28	0.25	0.39	0.33	0.25	0.21	0.31	0.23	0.06
μ (μ _B /atom)	2.00	1.50	1.00	0.80	0.40	1.33	0.33	2.29	0.29	1.56	0.22

Notation	P ₁₂	P ₁₆	P ₁₉	P ₂₀	¹ P ₂₅	² P ₂₅	P ₃₆	P _d	P _s
Structure									
Symmetry	D _{2h}	D _{4h}	D _{2h}	D _{2h}	C _{2h}	D _{4h}	D _{4h}	D _{2h}	D _{4h}
E _B (eV/atom)	3.69	3.77	3.82	3.88	3.93	3.98	4.06	4.56	4.58
E _G (eV)	0.04	0.10	0.06	0.08	0.09	0.18	0.12	0.00	0.00
(μ _B /atom)	0.50	0.50	0.42	0.30	0.96	0.32	0.17	1.08	0.08

*The results were taken from ref 28.

a binding energy of 2.59 eV/atom. The structural data of this relaxed trimer are shown in Table 2 together with its electro-magnetic properties.

As shown in Table 2, the triangular and square units are two building blocks in the formation of planar Ru clusters. Furthermore, results in Table 2 show that the Ru clusters that contain many square units, such as 2P_4 , 2P_5 , 2P_6 , 2P_7 , 2P_9 , and $^2P_{25}$, are more stable than their corresponding isomers that contain many triangular units, such as 1P_4 , 1P_5 , 1P_6 , 1P_7 , 1P_9 , and $^1P_{25}$. We mention that the square units in the $^1P_{25}$ cluster were initially set as triangular units, and they were relaxed to the current structure. These results demonstrate that the binding energies of the Ru planar clusters formed by square units are more stable than those formed by triangular units. An analysis of the results in Table 2 shows that the binding energy difference between the clusters of square units and their isomers of triangular units decreases with increasing cluster size. For instance, the binding energy difference between 2P_4 and 1P_4 is 0.36 eV/atom, which decreases to 0.20 eV/atom between 2P_9 and 1P_9 and further to 0.05 eV/atom between $^2P_{25}$ and $^1P_{25}$. The difference in binding energy between the infinite structures P_s and P_d becomes even smaller.

The binding energy of the infinite planar Ru structure is 68% of that of the Ru bulk. This result indicates that the planar Ru clusters are less relatively stable than the Pd planar clusters, as the binding energy of the infinite planar Pd cluster is 70% of that of the Pd bulk.²⁷ We also note that the infinite planar Pd cluster with triangular units, that is, P_d shown in Table 2, is substantially more stable than the P_s structure.²⁷

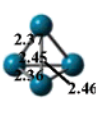
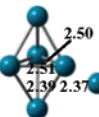
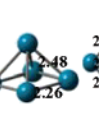
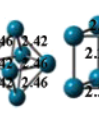
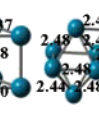
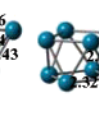
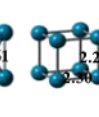
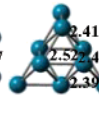

All the planar Ru clusters in Table 2 have rather small HOMO–LUMO band gaps of less than 0.41 eV, which indicates that they are good electrical conductors. They are also ferromagnetic. Furthermore, the less stable diamond-shaped Ru clusters, such as 1P_4 , 1P_9 , and $^1P_{25}$, have larger magnetic moments than the square-shaped ones, such as 2P_4 , 2P_9 , and $^2P_{25}$. Interestingly, 1P_7 has the largest magnetic moment among all the planar Ru clusters, which was also observed in our previous studies on the planar Pd clusters.²⁷ Finally, we point out that

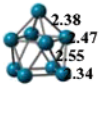
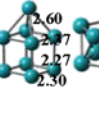
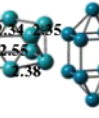
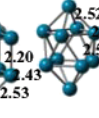
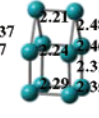
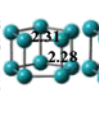
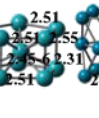
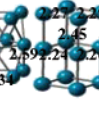


both of the infinite planar structures are ferromagnetic, which agrees with the experimental observation where the ruthenium monolayer deposited on graphite was found to be ferromagnetic.³⁰

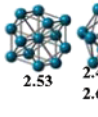
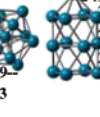
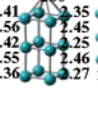
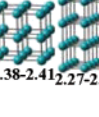
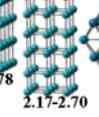
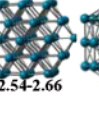
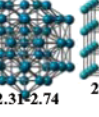
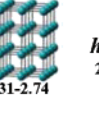
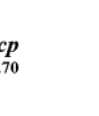


3.3. Three-Dimensional Ru Clusters. The structural information, binding energies, HOMO–LUMO band gaps, and magnetic moments of 29 three-dimensional ruthenium clusters up to 64 atoms as well as the Ru bulk are summarized in Table 3.

Before proceeding to discuss the results in Table 3, we first compare our results for the Ru bulk, the 13-atom cluster, and the 55-atom cluster with the results in the literature. The bond distance and binding energy for the ruthenium bulk from our calculations are 2.70 Å and 6.69 eV/atom, respectively, which are in good agreement with the experimental results of 2.65 Å and 6.74 eV/atom.²⁹ Our calculated bond distance for the $^1T_{13}$ cluster is 2.53 Å, which is slightly shorter than those of 2.59 Å¹¹ and 2.57 Å.¹⁷ The binding energy of the $^1T_{13}$ cluster is 4.04 eV/atom, which is between those of 3.75 eV/atom¹² and 4.27 eV/atom.¹⁵ The average bond distance for the $^2T_{13}$ cluster is 2.59 Å, which is slightly longer than the values of 2.54 Å¹¹ and 2.55 Å.¹⁷ The binding energy is 4.16 eV/atom, which is between those of 3.82 eV/atom¹² and 4.32 eV/atom.¹⁵ The binding energies for the $^1T_{55}$ and $^2T_{55}$ clusters are 5.14 and 5.19 eV/atom, respectively. These values are about 76% of the Ru bulk binding energy. Deng et al. reported binding energies of 6.56 eV/atom for the $^1T_{55}$ cluster and 6.45 eV/atom for the $^2T_{55}$ cluster,¹¹ whereas Guirado-López et al. reported a value of 6.00 eV/atom for the $^1T_{55}$ cluster.¹⁴ These values are particularly high if one compares them with the binding energy of the bulk (6.74 eV/atom). The magnetic moments of the $^1T_{13}$ and $^2T_{13}$ clusters are 1.08 and 1.00 μ_B /atom, respectively, which are in good agreement with Reddy et al.'s calculations.¹⁵ The magnetic moments of the $^1T_{55}$ and $^2T_{55}$ clusters are 0.18 and 0.25 μ_B /atom, respectively, which are slightly larger than those of 0.11 and 0.22 μ_B /atom reported by Deng et al.¹²

TABLE 3: Bond Distances (in Å), Binding Energies (E_B), HOMO–LUMO Band Gaps (E_G), and Magnetic Moments (μ) of Three-Dimensional Ru Clusters

Notation	T_4^*	1T_5	2T_5	1T_6	2T_6	T_7	1T_8	$^2T_8^*$	1T_9
Structure									
Symmetry	C_s	C_{2v}	C_{4v}	C_s	C_{2v}	C_s	C_{4v}	D_{4h}	C_s
E_B (eV/atom)	2.81	3.17	3.38	3.58	3.68	3.70	3.85	4.23	3.85
E_G (eV)	0.44	0.53	0.16	0.06	0.08	0.10	0.11	0.06	0.09
μ (μ_B /atom)	1.00	0.40	0.40	1.33	0.67	0.86	1.50	0.50	0.44

Notation	2T_9	$^3T_9^*$	$^1T_{10}$	$^2T_{10}$	$^3T_{10}$	$^4T_{10}$	$^5T_{10}$	T_{11}	$^1T_{12}$	$^2T_{12}^*$
Structure										
Symmetry	C_{4v}	C_{4v}	C_s	D_{4h}	C_{4v}	C_s	D_{5h}	C_{2v}	C_{4v}	C_{4v}
E_B (eV/atom)	4.00	4.18	3.85	4.04	4.08	4.23	4.27	4.17	4.24	4.40
E_G (eV)	0.19	0.16	0.09	0.18	0.51	0.11	0.07	0.31	0.05	0.09
μ (μ_B /atom)	0.90	0.90	1.60	0.60	0.40	0.60	0.80	0.18	0.67	0.17

Notation	$^1T_{13}^*$	$^2T_{13}^*$	$^3T_{13}$	$^4T_{13}^*$	T_{27}	T_{48}	T_{54}	$^1T_{55}$	$^2T_{55}$	T_{64}	Bulk
Structure											
Symmetry	O_h	C_s	C_{4v}	C_{4v}	D_{4h}	D_{4h}	D_{4h}	O_h	C_s	D_{4h}	hcp
E_B (eV/atom)	4.04	4.16	4.23	4.37	4.67	4.93	4.90	5.14	5.19	5.07	6.69
E_G (eV)	0.06	0.30	0.07	0.07	0.18	0.08	0.15	0.07	0.11	0.07	0.00
μ (μ_B /atom)	1.08	1.00	0.62	0.46	0.44	0.33	0.19	0.18	0.25	0.16	0.00

*The data were taken from ref 28.

We now focus on the correlation between the structure and stability of Ru clusters. The results for the planar Ru clusters discussed in the last subsection and shown in Table 2 indicate that square building blocks are substantially more stable than triangular building blocks. The above observation suggests that we may find simple cubic structures that are also stable, in addition to the structures that can be found from the bulk, such as the cubo-octahedral $^1T_{13}$ structure and the widely discussed icosahedral $^2T_{13}$ structure. The results in Table 3 show that this is indeed the case. First, the simple cubic structures, such as 2T_8 and $^2T_{12}$, were found to be the most stable isomers. Furthermore, the comparison between the T_{54} , $^2T_{55}$, and T_{64} clusters in Table 3 shows that the most stable structure is an icosahedron, which indicates that the simple cubic structure is no longer the most stable structure when the cluster size becomes larger than 55.

To explore the critical cluster size at which the structural change occurs, we plotted in Figure 1 the binding energy of the simple cubic, cubo-octahedral, and icosahedral clusters as a function of cluster size. In Figure 1 the dotted curve for the simple cubic structures crosses the solid and dashed lines, which represent the icosahedral and the cubo-octahedral structures, respectively, at about a cluster size of 40. This indicates that the simple cubic structure is the most stable one for clusters of less than about 40 atoms. Then the icosahedral structure becomes

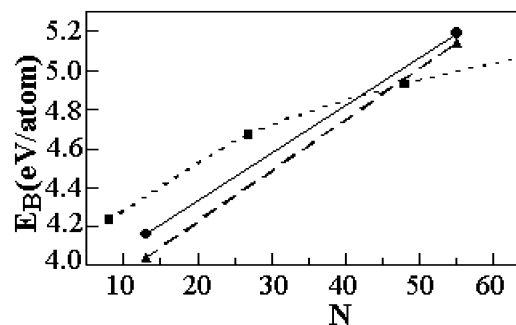


Figure 1. Binding energy (E_B) of simple cubic (■), cubo-octahedral (▲), and icosahedral (●) clusters as a function of cluster size (N).

the most stable one until at least 55 atoms. The difference in the binding energy between the $^2T_{55}$ and $^1T_{55}$ structure is 0.05 eV/atom and that between the $^2T_{13}$ and $^1T_{13}$ structure is 0.12 eV/atom. Following this tendency, it seems that a transition from the icosahedral to the cubo-octahedral structure might happen around the cluster of 147 atoms, in which Ru atoms form three closed-shells. After this, the cubo-octahedron structure becomes the most stable structure.

More interestingly, the results in Table 3 show that a disturbance to the perfect simple cubic structures can destabilize the cluster even though the cluster size increases by adding more Ru atoms. For instance, comparing 2T_8 , 3T_9 , and $^2T_{10}$ in Table

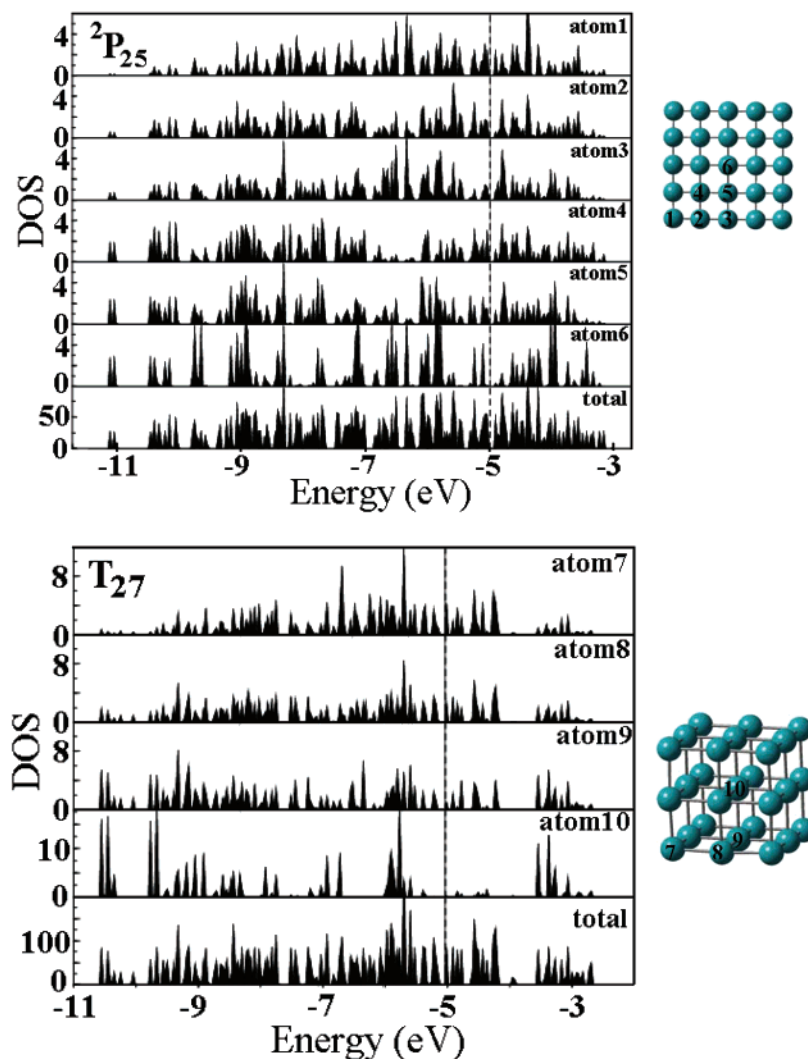


Figure 2. Density of states (DOS) of ${}^2P_{25}$ and its individual atoms (top) and the DOS of T_{27} and its individual atoms (bottom). The dashed lines denote the Fermi levels.

TABLE 4: Binding Energy of Building Blocks Used for Predicting the Binding Energy of a Ru Cluster^a

Notation	E_{sc}	E_{se}	E_{si}	E_{dc1}	E_{dc2}^*	E_{de}	E_{di}	E_{tc}	E_{ta}	E_{ts}	E_{ti}
Structure											
Bond length (Å)	2.22	2.30	2.38	2.20/2.37		2.46	2.55	2.27/2.30	2.38	2.37/2.47	2.51
E_B (eV/atom)	3.09	3.83	4.58	2.59	3.07	3.58	4.56	4.23	4.87	5.37	5.67

^a All the data shown here are based on the current DFT calculations. *The binding energy per atom for E_{dc2} was calculated by the binding energy difference between 1P_7 and E_{di} , i.e., $E_B = ((3.28)(7) - 4.56)/6 = 3.07$.

3, the binding energy decreases by adding one atom to the 2T_8 cluster, that is, 3T_9 , and decreases further by adding another atom to form ${}^2T_{10}$. Another very similar example is ${}^2T_{12}$, ${}^4T_{13}$, and T_{14} , which has D_{4h} symmetry (not shown in Table 3) and was constructed by adding one more atom beneath the bottom square of the ${}^4T_{13}$ cluster. The results in Table 3 show that the binding energy decreases from ${}^2T_{12}$ to ${}^4T_{13}$. The binding energy decreases further to 4.32 eV/atom for T_{14} . These results demonstrate that the simple cubic structure is the most stable structure in small three-dimensional ruthenium clusters. Although previous publications reported that the closed-shell cubo-octahedron and icosahedron are the most stable structures,^{11–14} our results show that the simple cubic-like ${}^4T_{13}$ is the most stable structure for Ru_{13} . Not only is the binding energy of the ${}^4T_{13}$ structure 0.21 eV higher than that of the icosahedral ${}^2T_{13}$

structure, but seven smaller clusters of simple cubic structures (2T_8 , 3T_9 , ${}^3T_{10}$, ${}^4T_{10}$, T_{11} , ${}^1T_{12}$, and ${}^2T_{12}$) were also found to be more stable than the icosahedral ${}^2T_{13}$.

All the three-dimensional Ru clusters shown in Table 3 have small HOMO–LUMO gaps of less than 0.53 eV, which indicates that they are good electrical conductors. These three-dimensional ruthenium clusters are also ferromagnetic. The magnetic moments of small ruthenium clusters with less than 13 atoms are higher than those of the Pd clusters²⁷ but are slightly lower than those of the Rh clusters.²⁶

3.4. Stability Prediction of Certain Planar and Simple Cubic Ru Clusters. The current DFT calculations were carried out on Linux workstations and in our 50-processor Beowulf cluster. It becomes difficult to carry out calculations for large clusters of more than 100 atoms because of the limitation of

TABLE 5: Comparison of the Binding Energy between the Predicted (E_p) and the DFT Results (E_B) of Ru Clusters

notation:	2P_6	1P_9	2P_9	P_{12}	${}^1P_{16}$	P_{20}	${}^1P_{25}$	${}^1P_{25}$	P_{36}	P_{900}	T_{27}	T_{48}	T_{54}	T_{64}
$m \times n$ or $l \times m \times n^a$	2×3	3×3	3×3	3×4	4×4	4×5	5×5	5×5	6×6	30×30	$3 \times 3 \times 3$	$3 \times 4 \times 4$	$3 \times 3 \times 6$	$4 \times 4 \times 4$
E_p (eV/atom)	3.34	3.36	3.58	3.71	3.83	3.91	3.81	3.98	4.08	4.48	4.82	5.00	5.00	5.08
E_B (eV/atom)	3.32	3.39	3.59	3.69	3.77	3.88	3.93	3.98	4.07		4.67	4.92	4.90	5.07

^a The terms m and n are the number of atoms in the two unparallel directions in planar clusters, respectively, and l , m , and n are the number of atoms in the x , y , and z directions in the simple cubic clusters, respectively.

computer memory and time. Therefore, it is important to explore whether we can predict the stability of larger clusters based on the data obtained for the small ones.

In our previous work on the Pd clusters²⁷ we used two parameters, that is, the binding energy for a triangular unit and that for a square unit, to predict the binding energies of large Pd clusters. The results show that they can predict the relative stability of Pd clusters qualitatively. Furthermore, the results for the Pd and Ru clusters indicate that atoms having similar bonding environments are quite similar. To provide further evidence for this, we plotted in Figure 2 the total density of states (DOS) and the DOS for individual atoms of different bonding environments of ${}^2P_{25}$ and T_{27} .

We discuss first the DOS for the ${}^2P_{25}$ cluster, which are shown in the top of Figure 2. The DOS distribution from atom 1 to atom 6 moves further below the Fermi level, which indicates an increase in the binding energy from atom 1 to atom 6. The same phenomenon was found for atoms in the T_{27} cluster. Furthermore, the center atoms in both clusters, that is, atom 6 or atom 10, have the largest band gap. These suggest that the electrons around the central atom are bound more strongly to the atom. More importantly, the other unlabeled atoms in these clusters have one of the DOS shown in Figure 2. Therefore, this illustrates that atoms with similar bonding environments have similar binding energy, and we can divide the atoms of the clusters into several smaller units.

For instance, in an $m \times n$ rectangular cluster, where m and n are the number of atoms in two perpendicular directions, there are three kinds of atoms: four atoms at the corner, $2(m + n - 4)$ atoms at the edge, and $(m - 2)(n - 2)$ atoms in the inside of the rectangular cluster. We use the following equation to estimate the binding energy of any rectangular planar ruthenium cluster,

$$E_p = [4E_{sc} + (2m + 2n - 8)E_{se} + (m - 2)(n - 2)E_{si}]/(mn) \quad (3)$$

where E_p is the predicted binding energy (in eV/atom) of a planar rectangular cluster, E_{sc} , E_{se} , and E_{si} are the binding energy of the corner, edge or inside atoms in the cluster, respectively, and their values are given in Table 4. The predicted results for some rectangular structures were summarized in Table 5. The comparison between the predicted and the DFT results in Table 5 shows that eq 3 can predict the stability of the rectangular clusters rather accurately.

To predict the stability of the diamond planar Ru clusters, we propose to use

$$E_p = [2(E_{dc1} + E_{dc2}) + (2m + 2n - 8)E_{de} + (m - 2)(n - 2)E_{di}]/(mn) \quad (4)$$

where m and n are the number of atoms in two unparallel directions, E_{dc1} and E_{dc2} are the binding energy of the corner atoms that are bonded to two and three other atoms, respectively, and E_{de} and E_{di} represent the binding energies of the edge atoms and inside atoms that are bonded to four and six other atoms, respectively. The values for E_{dc1} , E_{dc2} , E_{de} , and E_{di} are provided

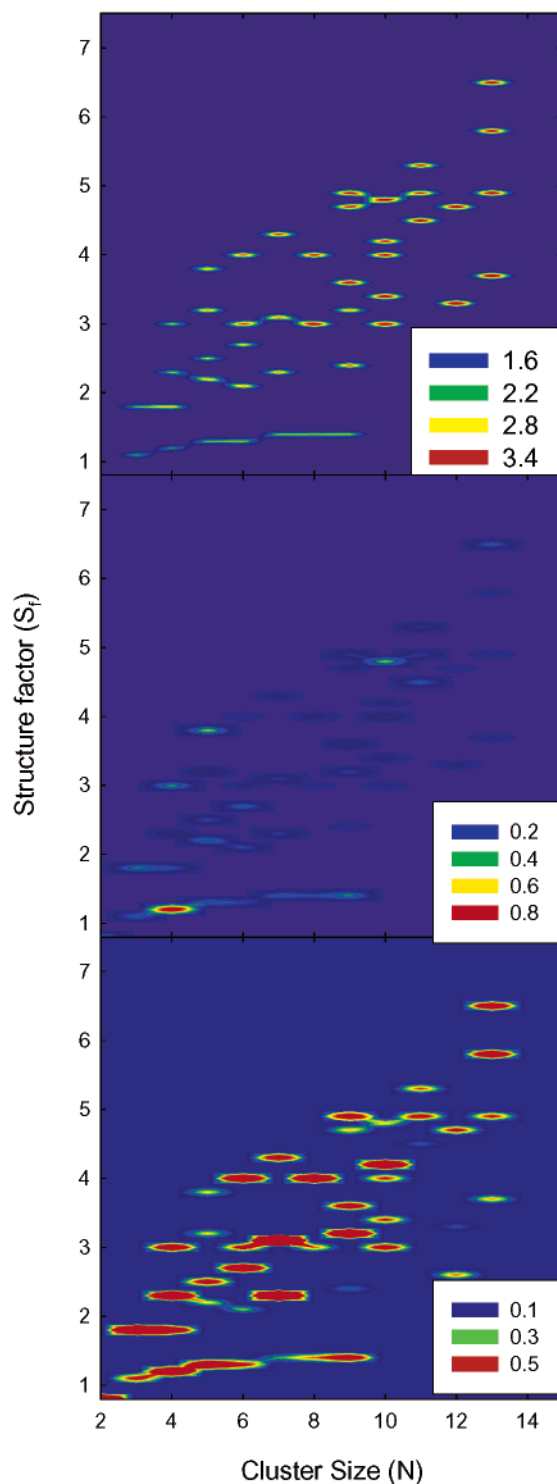


Figure 3. Contour plots of the binding energy (top), HOMO–LUMO band gap (middle), and magnetic moment (bottom) of Ru clusters as a function of cluster size (N) and structure factor (S_f).

in Table 4. The estimation of binding energy for 1P_9 and ${}^1P_{25}$ were made based on eq 4. The result for 1P_9 in Table 5

TABLE 6: Mulliken Population Analysis and the Magnetic Moments of Individual Ru Atoms in Four Clusters^a

notation		charge				neat charge	magnetic moment (μ_B)			
		4d* ^b	5s	4d _z ²	total		4d*	5s	4d _z ²	total
² P ₂₅	atom 1 (2) × 4	6.85	0.62	0.23	7.70	+0.30	0.93	0.12	0.01	1.06
	atom 2 (3) × 8	6.84	0.67	0.45	7.97	+0.03	0.18	0.03	0.02	0.23
	atom 3 (3) × 4	6.85	0.67	0.39	7.91	+0.09	-0.21	0.05	0.01	-0.15
	atom 4 (4) × 4	6.84	0.74	0.65	8.23	-0.23	0.13	0.03	0.01	0.17
	atom 5 (4) × 4	6.86	0.74	0.59	8.19	-0.19	0.17	0.02	0.01	0.20
T ₂₇	atom 6 (4) × 1	6.90	0.69	0.52	8.11	-0.11	-0.12	-0.01	0.01	-0.12
	atom 7 (3) × 8	6.75	0.64	0.29	7.69	+0.31	0.65	0.09	0.02	0.76
	atom 8 (4) × 12	6.78	0.69	0.50	7.96	+0.04	0.29	0.00	0.02	0.31
	atom 9 (5) × 6	6.84	0.73	0.71	8.28	-0.28	0.15	0.00	0.00	0.15
	atom 10 (6) × 1	6.99	0.77	0.95	8.70	-0.70	-0.14	0.00	0.02	-0.12
¹ T ₁₃	outer (5) × 8	6.83	0.64	0.45	7.92	+0.08	0.97	0.29	0.04	1.04
	outer (6) × 4	6.83	0.64	0.45	7.92	+0.08	0.97	0.29	0.04	1.04
	inner (12) × 1	6.93	0.82	1.23	8.98	-0.98	-0.43	-0.02	-0.04	-0.49
² T ₁₃	outer (6) × 12	6.84	0.64	0.45	7.93	+0.07	0.75	0.02	0.07	0.84
	inner (12) × 1	7.00	0.87	1.32	8.98	-0.98	-0.23	-0.02	-0.02	-0.27

^aThe numbers in parentheses are the coordination numbers of the atom, and the numbers following the × sign are the number of atoms that have the same properties as those labeled atoms. The labeled atoms in ²P₂₅ and T₂₇ are shown in Figure 2, and the terms inner and outer in ¹T₁₃ and ²T₁₃ represent the center atom and the shell atoms, respectively. There are two types of shell atoms in ¹T₁₃, i.e., atoms with a 5-coordination number and atoms with a 6-coordination number. ^bThe 4d* is the population without including the 4d_z² population.

demonstrates that the estimation is accurate. In the case of ¹P₂₅, the prediction underestimated the binding energy because of the use of the binding energy of triangular units to calculate the binding energy of the two square units in ¹P₂₅ (shown in Table 2).

Finally, we discuss the prediction of binding energy for simple cubic Ru clusters. Our prediction was made using

$$E_p = [8E_{ic} + 4(l + m + n - 6)E_{ta} + 2((l - 2)(m - 2) + (m - 2)(n - 2) + (l - 2)(n - 2))E_{ts} + (l - 2)(m - 2)(n - 2)5.67]/(lmn) \quad (5)$$

where l , m , and n represent the number of atoms in the x , y , and z directions, respectively. E_{ic} , E_{ta} , E_{ts} , and E_{ij} are the binding energy of the atoms in different bonding environments, which are shown in Table 4 together with their values. The predicted binding energies for four simple cubic Ru clusters are summarized in the last four columns of Table 5. These results show that the predicted binding energies are in good agreement with those from the DFT calculations.

3.5. Correlation between the Energetic and Electromagnetic Properties of Ru Clusters and the Cluster Size and Structure. Following our previous work on the Pd clusters,²⁷ we correlated in this work the binding energy, the HOMO–LUMO band gap, and the magnetic moment for the Ru clusters with size and structure. The structure factor, S_f , was used to quantify these Ru structures shown in Tables 1–3 and is calculated by

$$S_f = g_s g_d N_c \quad (6)$$

where \bar{N}_c is the coordination number per atom of the cluster, which is obtained by summing the coordination numbers for each Ru atom in the cluster and then dividing by the number of atoms in the cluster, that is, N . The two factors, g_s and g_d , were used to account for the symmetry and the dimensionality of the structure, respectively. For linear, planar, and three-dimensional structures, we set $g_d = 0.8$, 0.9 , and 1 , respectively. For all the clusters studied here, we set $g_s = 1$ except for ²T₉ and ¹T₁₀ for which we set $g_s = 1.05$.

The binding energies, the HOMO–LUMO band gaps, and the magnetic moments of Ru clusters of less than 13 atoms are plotted as a function of cluster size and structure factor in Figure 3. The top contour for the binding energy shows clearly that

many low-coordinated isomers, that is, simple cubic structures, are energetically possible. The middle contour shows how the HOMO–LUMO band gap changes with the cluster size and structure. It illustrates that Ru clusters are very good electrical conductors. The bottom plot in Figure 3 depicts the magnetic moments of the Ru clusters as a function of cluster size and structure. Nearly all the Ru clusters are ferromagnetic.

More interesting is the comparison between Figure 3 and Figure 5 for the Pd clusters in ref 27. The first observation is that the Ru clusters have small band gaps compared to those of the Pd clusters. This is reflected by the low intensity in the middle contour in Figure 3 compared to those of the Pd clusters. Second, the Ru clusters have higher magnetic moments regardless of their dimensionality, which was shown by the intense bright color throughout the bottom contour of Figure 3. In contrast, the linear Pd clusters tend to have high magnetic moments. This comparison shows that the clusters formed from different elements have different properties and can be characterized using Figure 3.

To further explore why the simple cubic structure is the most stable structure in small Ru clusters, we did a Mulliken population analysis. The charges and the magnetic moments of individual atoms for several Ru clusters are given in Table 6. Before we make comparisons among the clusters of different elements, we first focus on the discussion of the charge and magnetic distributions of individual atoms in the clusters shown in Table 6. The results show that the inner atoms, such as the center atom in ¹T₁₃ and ²T₁₃, the atoms labeled as 4, 5, and 6 of ²P₂₅, and the atoms labeled as 9 and 10 of T₂₇ in Figure 2, are all negatively charged, but the edge or the corner atoms in these clusters are positively charged. This indicates that the less-coordinated atoms in the cluster are positively charged, whereas the inner atoms are negatively charged. Furthermore, the existence of the positively charged atoms at the corner or the edge suggests that electron rich molecules, such as CO or benzene, will be easily adsorbed on these sites. On the other hand, the atoms consisting of the faces of the clusters, such as atoms 4, 5, and 6 in ²P₂₅ and atom 9 in T₂₇ (see Figure 2 and Table 6), will attract nucleophilic species.

The less-coordinated corner or the edge atoms in the Ru clusters have the largest magnetic moments, as shown in Table 6. Furthermore, for the three-dimensional Ru clusters, the magnetic moments of the inner atoms have an opposite sign

compared to the outer atoms, such as in $^1T_{13}$. The fact that the electrons of the inner and surface atoms have different spin together with the different magnitudes in magnetic moment may explain why the magnetic moment decreases at larger cluster size. The increase in cluster size means that the ratio of the inner to the outer atoms increases, thus canceling out the net magnetic moment of the Ru clusters.

The results on the charge distribution of individual atoms in the Ru cluster in Table 6 show that the largest difference in the charge distribution among atoms comes from the $4d_z^2$ population. For instance, the $4d_z^2$ population of an outer atom in $^2T_{13}$ is about 34% of that of the inner atom. This was also observed in the Pd clusters. Furthermore, the atoms in the simple cubic clusters, such as $^2P_{25}$ and T_{27} , have similar 5s populations, but the atoms in the clusters of having triangular units, such as the two 13-atom clusters shown in Table 6, have quite different 5s populations compared to those in $^2P_{25}$ and T_{27} . The outer atoms have only about 74% of the 5s population of the inner atom in $^1T_{13}$ and $^2T_{13}$.

4. Conclusions

A systematic investigation of Ru clusters was carried out using DFT with a plane wave basis set. The results have shown that the simple cubic structure is the most stable structure in the small ruthenium clusters. Analysis suggests that the simple cubic structure could be the most stable structure for clusters of up to 40 atoms, the icosahedron is the most stable structure for clusters of 40–147 atoms, and finally the cubo-octahedron, that is, the bulk structure, becomes the most stable structure for clusters of more than 147 atoms. A strong trend of trimer formation was found in linear ruthenium clusters. All the clusters investigated here have small HOMO–LUMO band gaps, which indicates that they are good electrical conductors. They are also ferromagnetic with large magnetic moments. A quantitative correlation was provided between the energetic, electronic, and magnetic properties of ruthenium clusters and the cluster structure and size. Analysis of the calculated binding energies indicates that the atoms in similar bonding environments have similar binding energies. On the basis of this analysis, estimations were made on the binding energies of planar and simple cubic ruthenium clusters. The estimated binding energies agree well with the DFT results.

Acknowledgment. W.Z. and H.Z. acknowledge the State Key Lab C1 Chemical Technology, Tianjin University, for

support. L.W. acknowledges the start-up fund from Southern Illinois University at Carbondale.

References and Notes

- (1) Miedema, A. R.; Gingerich, K. A. *J. Phys. B* **1979**, *12*, 2081.
- (2) Wang, H.; Liu, Y.; Haouari, H.; Craig, R.; Lombardi, J. R.; Lindsay, D. M. *J. Chem. Phys.* **1997**, *106*, 6534.
- (3) Cotton, F. A.; Shim, I. *J. Am. Chem. Soc.* **1982**, *104*, 7025.
- (4) Andzelm, J.; Rodzio, E.; Salahub, D. R. *J. Chem. Phys.* **1985**, *83*, 4573.
- (5) Kalyan, K. D.; Balasubramanian, K. *J. Chem. Phys.* **1991**, *95*, 2568.
- (6) Chen, H.; Krasowski, M.; Fitzgerald, G. J. *J. Chem. Phys.* **1993**, *98*, 8710.
- (7) Harada, M.; Dexpert, H. *J. Phys. Chem.* **1996**, *100*, 565.
- (8) Tsuneda, T.; Suzumura, T.; Hirao, K. *J. Comput. Chem.* **2001**, *22*, 1995.
- (9) Guo, R.; Balasubramanian, K. *J. Chem. Phys.* **2003**, *118*, 142.
- (10) Fang, L.; Shen, X.; Chen, X.; Lombardi, J. R. *J. Chem. Phys. Lett.* **2000**, *332*, 299.
- (11) Yang, J.; Deng, K.; Xiao, C.; Wang, K. *Phys. Lett. A* **1996**, *212*, 253.
- (12) Deng, K.; Yang, J.; Xiao, C.; Wang, K. *Phys. Rev. B* **1996**, *54*, 2191.
- (13) Guirado-López, R.; Spanjaard, D.; Desjonquères, M. C.; Aguilera-Granja, F. *J. Magn. Magn. Mater.* **1998**, *186*, 214.
- (14) Guirado-López, R.; Spanjaard, D.; Desjonquères, M. C. *Phys. Rev. B* **1998**, *57*, 6305.
- (15) Reddy, B. V.; Khanna, S. N.; Dunlap, B. I. *Phys. Rev. Lett.* **1993**, *70*, 3323.
- (16) Wildberger, K.; Stepanyuk, V. S.; Lang, P.; Zeller, R.; Dederichs, P. H. *Phys. Rev. Lett.* **1995**, *75*, 509.
- (17) Cox, A. J.; Louderback, J. G.; Apsel, S. E.; Bloomfield, L. A. *Phys. Rev. B* **1994**, *49*, 12295.
- (18) Jennison, D. R.; Schultz, P. A.; Sears, M. P. *J. Chem. Phys.* **1997**, *106*, 1856.
- (19) Hartke, B. *Angew. Chem., Int. Ed.* **2002**, *41*, 1468.
- (20) Payami, M. *J. Chem. Phys.* **1999**, *111*, 8344.
- (21) Kresse G.; Hafner, J. *Phys. Rev. B* **1993**, *47*, 558.
- (22) Kresse G.; Furthmüller, J. *Phys. Rev. B* **1996**, *54*, 11169.
- (23) Kresse G.; Furthmüller, J. *Comput. Mater. Sci.* **1996**, *6*, 15.
- (24) (a) Vanderbilt, D. *Phys. Rev. B* **1990**, *41*, 7892. (b) Perdew, J. P.; Chevary, J. A.; Vosko, S. H.; Jackson, K. A.; Pederson, M. R.; Singh, D. J.; Fiolhais, C. *Phys. Rev. B* **1992**, *46*, 6671.
- (25) Perdew, J. P.; Chevary, J. A.; Vosko, S. H.; Jackson, K. A.; Pederson, M. R.; Singh, D. J.; Fiolhais, C. *Phys. Rev. B* **1992**, *46*, 6671.
- (26) Wang, L.; Ge, Q. *J. Chem. Phys. Lett.* **2002**, *366*, 368.
- (27) Zhang, W.; Wang, L.; Ge, Q. *J. Chem. Phys.* **2003**, *118*, 5793.
- (28) Zhang, W.; Xiao, L.; Hirata, Y.; Pawluck, T.; Wang, L. *J. Chem. Phys. Lett.* **2003**, *383*, 67.
- (29) Kittel, C. *Introduction to Solid-State Physics*, 5th ed.; Wiley: New York, 1976; p 74.
- (30) Pfandzelter, R.; Steierl, G.; Rau, C. *Phys. Rev. Lett.* **1995**, *74*, 3467.